



Published in final edited form as:

Cancer Res. 2013 December 1; 73(23): 6998–7008. doi:10.1158/0008-5472.CAN-13-0940.

Contribution of Bcl-2 Phosphorylation to Bak Binding and Drug Resistance

Haiming Dai^{#1,2}, Husheng Ding^{#1}, X. Wei Meng^{1,2}, Sun-Hee Lee¹, Paula A. Schneider¹, and Scott H. Kaufmann^{1,2}

¹Division of Oncology Research, Department of Oncology, Mayo Clinic, Rochester, MN 55905

²Department of Molecular Pharmacology and Experimental Therapeutics, Mayo Clinic, Rochester, MN 55905

These authors contributed equally to this work.

Abstract

Bcl-2 is phosphorylated on Ser⁷⁰ after treatment of cells with spindle poisons. Based on the cellular effects of overexpressing Bcl-2 S70E or S70A mutants, various studies have concluded that Ser⁷⁰ phosphorylation either enhances or diminishes Bcl-2 function. In the present study, the ability of phosphorylated Bcl-2, as well as the S70E and S70A mutants, to bind and neutralize proapoptotic Bcl-2 family members under cell-free conditions and in intact cells was examined in an attempt to resolve this controversy. Surface plasmon resonance indicated that phosphorylated Bcl-2, Bcl-2 S70E and Bcl-2 S70A exhibit enhanced binding to Bim and Bak compared to unmodified Bcl-2. This enhanced binding reflected a readily detectable conformation change in the loop domain of Bcl-2. Further, Bcl-2 S70E and S70A bound more Bak and Bim than wildtype Bcl-2 in pulldowns and afforded greater protection against several chemotherapeutic agents. Importantly, binding of endogenous Bcl-2 to Bim also increased during mitosis, when Bcl-2 is endogenously phosphorylated; and disruption of this mitotic Bcl-2/ Bim binding with navitoclax or ABT-199, like Bcl-2 downregulation, enhanced the cytotoxicity of paclitaxel. Collectively these results provide not only a mechanistic basis for the enhanced anti-apoptotic activity of phosphorylated Bcl-2, but also an explanation for the ability of BH3 mimetics to enhance taxane sensitivity.

Keywords

Apoptosis; mitosis; BH3 mimetic; drug resistance; CDK1

INTRODUCTION

Bcl-2 family members regulate apoptosis by controlling mitochondrial outer membrane permeabilization (1, 2). In particular, the proapoptotic multidomain Bcl-2 family members Bax and Bak are thought to directly permeabilize the outer mitochondrial membrane. Bax

Address correspondence to: Scott H. Kaufmann, M.D., Ph.D., or Haiming Dai, Ph.D. Division of Oncology Research Gonda 19-205 Mayo Clinic 200 First St., S.W. Rochester, MN 55905 Telephone: (507) 284-8950 Fax: (507) 293-0107 Kaufmann.Scott@Mayo.edu or Dai.Haiming@Mayo.edu.

Conflict of interest: The authors have no conflict of interest to report

AUTHOR CONTRIBUTIONS

S.H.K. and H. Dai designed the study. H. Dai, H. Ding, X.W. Meng, P. Schneider and S-H. L. performed and interpreted experiments. S.H.K. and H. Dai wrote the paper, which was edited by all authors.

and Bak are held in check by binding to the antiapoptotic Bcl-2 family members Bcl-x_L, Mcl-1, Bcl-w, and A1 as well as Bcl-2 itself. These interactions are further modulated by BH3-only proteins such as Bim, Puma, Bid, Noxa, Bik, Bad and Bmf, which are activated by various cellular stresses and then facilitate apoptosis by neutralizing antiapoptotic family members and, at least in the case of Bid, Bim and Noxa, by directly activating Bax and/or Bak.

Not all of the antiapoptotic Bcl-2 family members interact equally well with Bax and Bak. Even though the first paper describing Bak showed that it could be pulled down with Bcl-2 (3), subsequent studies have reported that Bak binds Mcl-1 and Bcl-x_L preferentially (4, 5). On the other hand, our previous studies demonstrated an equilibrium dissociation constant of ~150 nM for the Bcl-2·Bak complex and demonstrated that a sizable fraction of the total cellular Bak in certain lymphoid cell lines, particularly those with Bcl-2 overexpression, could be pulled down with endogenous Bcl-2 (6).

Additional experiments examined the potential role of phosphorylation in the protective effects of Bcl-2. Early studies not only identified Bcl-2 as a phosphoprotein (7) that is preferentially modified during mitosis (8, 9), but also suggested that paclitaxel treatment might inactivate Bcl-2 through this posttranslational modification (10, 11). In particular, it was reported that Bcl-2 S70A protected cells better than wildtype (wt) Bcl-2, raising the possibility that Bcl-2 Ser⁷⁰ phosphorylation inhibits Bcl-2 function (12). In contrast, other studies have demonstrated that phosphomimetic mutants with glutamate substituted at amino acids Thr⁶⁹, Ser⁷⁰, and Ser⁸⁷ also exhibit enhanced antiapoptotic effects, leading to the suggestion that phosphorylation enhances the activity of Bcl-2 (13, 14). Although it was suggested that these conflicting observations might reflect context-dependent effects of Bcl-2 phosphorylation (15), the mechanistic basis for either the proposed inactivation of Bcl-2 or its hyperactivation by phosphorylation remains unclear. Moreover, while several studies implicated cyclin-dependent kinase 1 (CDK1) as at least one possible Bcl-2 kinase (8, 16), others reported an inability of CDK1 to phosphorylate Bcl-2 *in vitro* (12, 17).

Previous studies have also shown that ABT-737 and navitoclax, which antagonize the effects of Bcl-2, Bcl-x_L and Bcl-w, dramatically sensitize a variety of cells to the cytotoxic effects of paclitaxel (18-22). These observations have led to at least two trials of navitoclax/taxane combinations (<http://www.clinicaltrials.gov/>). Based largely on correlations between Bcl-x_L expression and sensitivity to taxanes, it has also been suggested that the synergy between paclitaxel and ABT-737 or navitoclax reflects inhibition of Bcl-x_L. The possibility that a form of Bcl-2 present mainly during mitosis plays an important role in taxane sensitivity has not been investigated.

To resolve these issues, the present study was designed to determine whether phosphorylation inhibits or enhances the antiapoptotic function of Bcl-2, examine the mechanistic basis for the altered Bcl-2 function, and assess the impact of Bcl-2 phosphorylation on anticancer drug sensitivity. Results of this analysis demonstrated that phosphorylated Bcl-2 or the S70E mutant not only bound Bak and Bim with higher affinity under cell-free conditions, but also sequestered more Bim and Bak in intact cells, leading to enhanced protection against apoptosis. Interestingly, the Bcl-2 S70A mutant afforded similar protection, supporting a model in which Bcl-2 phosphorylation drives Bcl-2 to a more active conformation rather than providing a charge modification required for interaction with a phosphopeptide-directed binding partner.

MATERIALS AND METHODS

Materials

Reagents were obtained from the following suppliers: CM5 biosensor chips and Polysorbate 20 from GE Healthcare, Q-VD-Oph from SM Biochemicals (Anaheim, CA), glutathione (GSH) and paclitaxel from Sigma, GSH-agarose and trypsin-TPCK from Thermo Scientific, navitoclax and ABT-199 from Chemietek, activated CDK1/cyclin B complex from Millipore, Ni²⁺-NTA-agarose from Novagen, and allophycocyanin (APC)-conjugated annexin V from BD Biosciences. Antibodies to the following antigens were purchased from the indicated suppliers: Bcl-2 from Dako; Bax, Bim, Bcl-x_L, Mcl-1, green fluorescent protein (GFP) and glyceraldehyde phosphate dehydrogenase (GAPDH) from Cell Signaling Technology; Bak and Ser⁷⁰-Bcl-2 from Millipore; and actin (goat polyclonal) and Puma (rabbit polyclonal) from Santa Cruz Biotechnology. Anti-S peptide antibody was raised in our laboratory as described (23). The 26-mer Bim BH3 peptide (RPEIWIAQELRRIGDEFNAYYARRVF) was generated by solid phase synthesis in the Mayo Clinic Proteomics Research Center (Rochester, MN).

Protein expression and purification

Plasmids encoding His₆-tagged Bak Δ TM (GenBank BC004431, residues 1-186) in pET29b(+) and glutathione-S-transferase- (GST-) tagged Bcl-2 Δ TM have been described previously (6). cDNA encoding Bcl-2 Δ TM (GenBank BC027258, residue 1-219) was also cloned into pET29a(+), generating the Bcl-2 Δ TM protein with a C terminal His₆-tag. Plasmids encoding Bcl-2 mutants were generated using site-directed mutagenesis. All plasmids were subjected to automated sequencing to verify the described alteration and confirm that no additional mutations were present.

To express tagged Bak Δ TM or Bcl-2 Δ TM, plasmids were transformed into *E. coli* BL21 by heat shock. After cells were grown to an optical density of 0.8, 1 mM IPTG was added to induce protein synthesis at 18 °C for 24 h. Bacteria were then washed and sonicated on ice in TS buffer [150 mM NaCl containing 10 mM Tris-HCl (pH 7.4) and 1 mM freshly added PMSF]. All further steps were performed at 4 °C.

After His₆-tagged proteins were applied to Ni²⁺-NTA-agarose, columns were washed with 20 volumes of TS buffer followed by 10 volumes TS buffer containing 40 mM imidazole and eluted with TS buffer containing 200 mM imidazole. After GST-tagged proteins were incubated with GSH-agarose for 4 h, beads were washed twice with 20-25 volumes of TS buffer and eluted with TS containing 20 mM GSH for 30 min at 4 °C.

Fast protein liquid chromatography (FPLC)

Bcl-2 Δ TM-His₆, either wt or mutant, were further purified by FPLC on a mono Q column with buffer A (50 mM Na₂HPO₄, pH 8.5) and buffer B (50 mM Na₂HPO₄, 1 M NaCl, pH 8.5). The Bcl-2 Δ TM-containing fractions were subjected to SDS-PAGE.

In vitro phosphorylation and mass spectrometry

In order to achieve a high degree of modification, 100 μ g purified Bcl-2 Δ TM-His₆ was incubated with 5 μ g purified CDK1/cyclin B complex at 30 °C for 2 h in buffer containing 1 mM ATP, 1 mM MgCl₂, 150 mM NaCl, and 20 mM HEPES (pH 7.4). Aliquots of the reaction mixture were subjected to SDS-PAGE, transferred to nitrocellulose and stained with fast green, blotted with anti-phospho-Ser⁷⁰-Bcl-2 or subjected to liquid chromatography (LC) on an Agilent 1200 LC system coupled to electrospray ionization and time-of-flight mass spectrometry (MS) on an Agilent 6224 TOF mass spectrometer (Mayo Clinic Proteomics Core Facility, Rochester, MN). Alternatively, aliquots of the same sample

were also subjected to trypsin digestion followed by nano-LC/MS/MS using an Eksigent nano-LC-2D HPLC system (Eksigent, Dublin, CA) coupled to a Thermo Scientific Orbitrap Elite Hybrid Mass Spectrometer (Thermo Fisher Scientific, Bremen, Germany) to identify phosphorylation sites.

Trypsin digestion

After 2.5 μg Bcl-2 ΔTM -His₆ (wt, S70A, S70E) was incubated with 5 ng Trypsin-TPCK in HEPES buffer (150 mM NaCl, 20 mM HEPES, pH 7.4) for 30 min at 30°C, the reaction products were subjected to SDS-PAGE and stained with Coomassie blue G-250. An aliquot of trypsin-digested Bcl-2 ΔTM -His₆ S70A was subjected to liquid chromatography coupled with electrospray ionization and time-of-flight mass spectrometry as described above to identify the two tryptic cleavage fragments.

Surface plasmon resonance (SPR)

Proteins for SPR were further purified by FPLC on Superdex S200, concentrated in a centrifugal concentrator (Centricon, Millipore), dialyzed against Biacore buffer [10 mM HEPES (pH 7.4), 150 mM NaCl, 0.05 mM EDTA and 0.005% (w/v) Polysorbate 20] and stored at 4 °C for <48 h before use.

Bak ΔTM or 26mer Bim BH3 peptide (24) was immobilized on a CM5 chip using a Biacore T200 biosensor. Binding assays were performed at 25 °C using Biacore buffer containing GST or GST-Bcl-2 ΔTM (wt or mutant) or Bcl-2 ΔTM -His₆ (phosphorylated or unmodified) injected at 30 $\mu\text{l}/\text{min}$ for 1 or 2 min. Bound protein was allowed to dissociate in Biacore buffer at 30 $\mu\text{l}/\text{min}$ for 10 min and then desorbed with 20 mM Glycine (pH 2). Binding kinetics were derived using BIA Evaluation software (Biacore, Uppsala, Sweden).

Cell culture, transfection and drug treatment

K562 and Jurkat cells were maintained at densities below 5×10^5 cells/ml in RPMI 1640 medium containing 10% heat-inactivated fetal bovine serum, 100 units/ml penicillin G, 100 $\mu\text{g}/\text{ml}$ streptomycin, and 2 mM glutamine (Medium A) and passaged less than three months before being reinitiated from frozen stocks. Ovar5 and Ovar8 cells from NCI Frederick (25) or A2780 cells from T. Hamilton (Fox Chase Cancer Center, Philadelphia, PA) were maintained at <80% confluence in Medium A without (Ovar5, Ovar8) or with (A2780) 10 $\mu\text{g}/\text{ml}$ insulin. After cells were treated with paclitaxel in the absence or presence of navitoclax or ABT-199 for 24 or 48 h as indicated in the individual figures, cells were harvested for assays of apoptosis, which were performed as previously described (6). All cell lines were authenticated by short tandem repeat profiling in the Mayo Advanced Genomics Technology Center, most recently in July, 2012 and April, 2013.

To compare the ability of various Bcl-2 constructs to protect cells, log phase K562 cells were transiently transfected with plasmids encoding wt or mutant full-length Bcl-2 (40 μg) together with plasmid encoding EGFP-Histone H2B (5 μg) using a BTX 830 square wave electroporator delivering a single 320-V pulse for 10 msec. After incubation to allow transgene exposure, cells were treated with drugs or solvent as indicated in the figures. At the completion of the incubation, cells were sedimented at $50 \times g$, reacted with APC-conjugated annexin V and analyzed on a Becton Dickinson FACS Canto II flow cytometer (Becton Dickinson, Mountain View, CA) using the following lasers and filters: EGFP, 488 nm laser, 530/30 filter; APC, 633 nm laser, 660/20 filter. After collection of 20,000 events, APC-annexin V binding to the EGFP-positive cells was determined using Becton Dickinson Cell Quest software.

To evaluate the effects of downregulating various Bcl-2 family members, log phase K562 cells growing in antibiotic-free medium were electroporated with previously described siRNAs (6) targeting Bim, Puma, Bak or Bax (1 μ M). To knock down antiapoptotic Bcl-2 family members, we used two previously described shRNAs against Bcl-2 or Mcl-1 (6, 26), Bcl-x_L shRNA #1 generated by inserting the hairpin sequence of Huang (26) into the pCMS5A plasmid, or Bcl-x_L shRNA #2 from Jin-san Zhang (Mayo Clinic, Rochester, MN). The targeted sequences were: Bcl-2 #1: 5'-TGGATGACTGAGTACCTGAAC-3', Bcl-2 #2: 5'-ATGGCGCACGCTGGGAGAACG-3', Bcl-x_L #1: 5'-CAGGGACAGCATATCAGAG-3', Bcl-x_L #2: 5'-GTGGA ACTCTATGGGAACAAT-3', Mcl-1 #1: 5'-CGGGACTGGCTAGTTAAAC-3' and Mcl-1 #2: 5'-GATTGTGACTCTCATTCT-3'. Beginning 24 h after transfection, cells were treated with paclitaxel and/or navitoclax as indicated and assayed for annexin V binding by flow microfluorimetry as described above.

Pull-down assays

Using a 240-V pulse for 10 msec, log phase Jurkat cells growing in antibiotic free medium were transiently transfected with plasmids encoding full-length Bcl-2 (wt, S70A or S70E) fused at its N-terminus with the S peptide tag (6, 23). After 24 h, cells were washed and lysed in CHAPS buffer [1% CHAPS, 1% glycerol, 150 mM NaCl, 20 mM HEPES (pH 7.5) containing 1 mM freshly added PMSF, 10 μ g/ml leupeptin, 10 μ g/ml pepstatin, 100 mM NaF, 10 mM sodium pyrophosphate, 1 mM sodium vanadate and 20 nM microcystin] at 4°C for 30 min. Following clarification at 14,000 \times g, the supernatants were incubated with S protein-agarose for 24 h at 4°C. Beads were then washed four times with isotonic wash buffer containing 1% (w/v) CHAPS; and bound proteins were solubilized in SDS sample buffer, subjected to SDS-PAGE, and probed with the indicated antibodies. Bound antibodies were detected using peroxidase-coupled secondary antibodies and Thermo enhanced chemiluminescence reagents (27). The resulting x-ray images were imported into Photoshop on an Epson 4490 scanner, converted into PICT files without contrast adjustment, and assembled into figures in Canvas X.

To assess the effects of paclitaxel and navitoclax, K562 stably expressing S peptide-tagged Bcl-2 at levels equal to endogenous Bcl-2 were generated as previously described (28). Following treatment with 25 nM paclitaxel and/or 1 mM navitoclax for 18 h, cells were washed with PBS, and lysed in CHAPS buffer. After lysates were clarified, aliquots containing 600 μ g protein (assayed by the bicinchoninic acid method— ref. 29) were incubated with S protein-agarose for pulldowns as described in the preceding paragraph.

Statistical analysis

Graphs show summarized results from three independent experiments. Differences between treatments were analyzed by analysis of variance (ANOVA) using StatView5 (SAS). All *p* values stated in figure legends have been subjected to a Bonferroni correction (30).

RESULTS

Bcl-2 Ser⁷⁰ phosphorylation enhances Bcl-2/Bak and Bcl-2/Bim interactions

To assess the potential impact of Bcl-2 phosphorylation, purified Bcl-2 was treated with CDK1/cyclin B1 complex and assayed for binding to immobilized Bak using surface plasmon resonance, a well established method for studying protein-protein interactions (31, 32). Mass spectrometry demonstrated that Bcl-2 was phosphorylated on Thr⁶⁹, Ser⁷⁰, Thr⁷⁴, and Ser⁸⁷ by CDK1. Under the conditions of the reactions, very little unmodified Bcl-2 remained (Fig. 1A and S1). After CDK1/cyclin B-mediated modification, surface plasmon resonance indicated that Bcl-2 bound to Bak equally rapidly but dissociated more slowly

than unmodified Bcl-2 (Fig. 1B). Compared to an equilibrium dissociation constant (K_D) of ~150 nM for unphosphorylated Bcl-2 binding to Bak, phosphorylated Bcl-2 bound about 5-fold more tightly, although an accurate K_D could not be determined because the binding reflected multiple different phosphorylated species.

Further analysis demonstrated that mutation of Ser⁷⁰, a known site for phosphorylation by multiple kinases (33, 34), to the phosphomimetic amino acid glutamate also enhanced the affinity of purified Bcl-2 for Bak (Fig. 1C-F). Interestingly, mutation of Ser⁷⁰ to alanine had a similar effect (Fig. 1E), as indicated by the slower dissociation of Bcl-2 S70E and S70A from Bak (Fig. 1F). These results raised the possibility that the effect of modification at this site does not require the introduction of a negative charge.

In further studies, the effect of these mutations on binding to Bim, an important activator of apoptosis (35-37), was likewise examined. Wildtype Bcl-2 bound to Bim with a K_D of 7 nM, whereas Bcl-2 S70E and Bcl-2 S70A bound with K_D s of 0.1 nM and 1 nM, respectively (Fig. 1G-I), again demonstrating that modified Bcl-2 has a higher affinity for the proapoptotic protein.

Loop mutations alter Bcl-2 conformation

Because Thr⁶⁹, Thr⁷⁴ and Ser⁸⁷ are also phosphorylated by CDK1 *in vitro* (Fig. S1), we examined the impact of mutating these residues to alanine or glutamate as well. As shown in Fig. S2, each of these mutations also enhanced the binding of Bcl-2 to Bak under cell-free conditions. These results suggested that modification at any of the four sites is sufficient to affect binding and, because the altered function does not require introduction of a negative charge, that altered function might reflect a process that is independent of the generation of a phosphoepitope at a particular amino acid. Further experiments focused on Ser⁷⁰, the most intensively studied but also most controversial phosphorylation site (see Introduction).

Because Ser⁷⁰ is located in an unstructured region of the Bcl-2 protein, this portion of the protein has been deleted in previous constructs used to determine the Bcl-2 three-dimensional structure (18, 38, 39). Accordingly, it is impossible to assess the detailed effects of Ser⁷⁰ mutations on Bcl-2 conformation. On the other hand, while purifying Bcl-2 S70A and S70E, we observed increased proteolysis of these proteins in bacterial lysates compared to wt Bcl-2 (Fig. S3A). Moreover, when FPLC fractions containing full-length Bcl-2 S70A and S70E were subjected to limited proteolysis with trypsin, a procedure that has previously been used to assess changes in protein conformation (40), increased protease susceptibility was again observed (Fig. S3B). Mass spectrometry indicated that the Bcl-2 fragment arising from this *in vitro* proteolysis has been preferentially cleaved at Arg⁶⁸ (Fig. S3C), providing evidence that Bcl-2 “flexible loop domain” is in a conformation that relatively inaccessible to interaction with other proteins (as exemplified by trypsin) in wt Bcl-2 protein and is rendered more accessible by the S70E and S70A mutations.

Ser⁷⁰ modification increases Bak binding and survival in intact cells

To determine whether the changes in binding detected under cell-free condition would also be observed in intact cells, plasmids encoding wt Bcl-2, Bcl-2 S70A or Bcl-2 S70E were transiently transfected into Jurkat T cell ALL cells, a cell line chosen because prior studies have demonstrated the constitutive presence of Bcl-2/Bak complexes in these cells (6). The three constructs were expressed equally (Fig. 2A, lanes 6-8), ruling out a major change in protein stability. Consistent with the results in Fig. 1, increased amounts of Bak and, to a smaller extent, Bim, were detected bound to Bcl-2 S70A and S70E compared to wt Bcl-2 (Fig. 2A, lanes 3 and 4 vs. 2).

To determine whether the increased affinity of Bcl-2 S70E for Bak and Bim resulted in increased cellular protection, Jurkat cells were transfected with empty vector, wt Bcl-2, or S70 mutants along with EGFP-Bak or EGFP-Bim_{EL}. As indicated in Figs. 2B, 2C and S4, transfection with EGFP-Bak induced apoptosis in $55 \pm 7\%$ (mean \pm SD, 3 independent experiments) of cells co-transfected with empty vector. This was decreased to $40 \pm 3\%$ of cells by co-transfection with wt Bcl-2 but decreased further to $24 \pm 3\%$ by co-transfection with Bcl-2 S70E. Protection by Bcl-2 S70A was similar. Likewise, co-transfected Bcl-2 S70E and S70A protected cells more effectively than wt Bcl-2 when cells were transfected with EGFP-Bim_{EL} (Figs. 2C and S4). Similar effects were also observed in other cells as well, including mouse embryo fibroblasts (Fig. S5).

In further experiments, the ability of wt Bcl-2 versus Bcl-2 S70E to protect from drug-induced apoptosis was examined. When Jurkat cells were treated with $50 \mu\text{M}$ etoposide, an agent previously shown to trigger apoptosis through the mitochondrial pathway (41), transfection with wt Bcl-2 diminished the apoptosis from $43 \pm 5\%$ to $33 \pm 4\%$ of transfected cells, whereas Bcl-2 S70A and S70E at similar levels (inset, Fig. 3B) further decreased apoptosis to $23 \pm 1\%$ and $21 \pm 2\%$ of transfected cells (Fig. 3B). Likewise, induction of apoptosis by the farnesyltransferase inhibitor tipifarnib, an agent previously shown to induce apoptosis in lymphoid cells in a Bim- and Bak-dependent manner (41), was decreased more by Bcl-2 S70A and S70E than by wt Bcl-2 (Fig. 3C).

Implications of Bcl-2 phosphorylation for paclitaxel/navitoclax synergy

To further assess the impact of Bcl-2 phosphorylation, we examined conditions where Bcl-2 is phosphorylated in intact cells. In particular, treatment of K562 cells with 25 nM paclitaxel, which induced mitotic arrest of $>60\%$ of the cells (Fig. 4A, left panel), caused near-maximal phosphorylation of Bcl-2 *in situ* (Fig. 4A, right panel). This paclitaxel-induced Bcl-2 phosphorylation rapidly diminished (Fig. 4B, lanes 5-8) after addition of the CDK inhibitor flavopiridol (42), suggesting that CDK1 plays a role in this modification *in situ*. After paclitaxel treatment, increased Bak was detected in Bcl-2 immunoprecipitates (Fig. 4C, lane 2 vs. lane 1). Interestingly, total cellular Bim_{EL} diminished in this assay (Fig. 4C, lane 6), but the amount pulled down with Bcl-2 in paclitaxel-treated cells was unchanged (Fig. 4C, lane 2 vs. lane 1), suggesting an increase in affinity for Bim as well.

To assess the potential importance of this Bcl-2/Bim and Bcl-2/Bak binding, we examined the effect of Bcl-2 downregulation on paclitaxel-induced cell cycle changes and apoptosis. In these studies, Bcl-2 shRNA markedly enhanced the sensitivity of K562 cells to paclitaxel-induced apoptosis (Figs. 4D, S6 and S7) without any discernible effect on paclitaxel-induced mitotic arrest (Fig. 4E). This sensitizing effect of Bcl-2 knockdown was particularly noticeable at low paclitaxel concentrations (Figs. 4D and S7). Similar effects were observed with Bcl-x_L shRNA (Figs. 4D, S6 and S7), suggesting that Bcl-2 and Bcl-x_L both inhibit apoptosis during paclitaxel treatment. In contrast, Mcl-1 shRNA had a much more limited effect on paclitaxel-induced apoptosis.

In further experiments, we examined the action of navitoclax, a BH3 mimetic that displaces proapoptotic Bcl-2 family members from Bcl-2 and Bcl-x_L (43), in the absence and presence of paclitaxel. Paclitaxel by itself induced little apoptosis in K562 cells (Fig. 5A, B). In contrast, navitoclax markedly enhanced paclitaxel-induced apoptosis (Fig. 5A,B) that was Bim- and Bax-dependent (Fig. 5C). Similarly, in A2780 ovarian cancer cells, treatment with paclitaxel induced little apoptosis by itself, as did navitoclax, whereas the combination induced apoptosis in just under half of the cells (Fig. 5D, E), consistent with previous reports that ABT-737 or navitoclax sensitizes cells to paclitaxel (18-22). Similar sensitization was also observed in Ovar5 and Ovar8 cells (Fig. S8).

To assess whether this sensitization reflected effects of navitoclax on Bcl-2 or Bcl-x_L, cells were treated with paclitaxel in the absence or presence of the Bcl-2-selective BH3 agonist ABT-199 (44). As indicated in Figs. 5F and 5G, ABT-199 enhanced the cytotoxicity of paclitaxel, although the effects were somewhat smaller (Fig. S9; see also Fig. 5G vs. 5B and 5D). Accordingly, it appears that the navitoclax-induced sensitization to paclitaxel reflects, at least in part, antagonism of Bcl-2, although effects of Bcl-x_L were also evident.

DISCUSSION

The present results demonstrate that phosphorylated Bcl-2 as well as Bcl-2 S70E and S70A exhibit increased affinity for the proapoptotic proteins Bak and Bim. Consistent with these observations, increased sequestration of Bak and Bim is observed in cells transfected with Bcl-2 S70E or S70A as well as in cells where Bcl-2 becomes endogenously phosphorylated during paclitaxel treatment. The importance of this enhanced binding between phosphorylated Bcl-2 and its proapoptotic binding partners is demonstrated not only by the increased ability of Bcl-2 S70E to protect against various chemotherapeutic agents, but also by the marked increase in paclitaxel sensitivity observed when Bcl-2 is downregulated by shRNA. These results contribute new insight into regulation of Bcl-2 and simultaneously provide an explanation for the incompletely understood synergy between paclitaxel and BH3 mimetics.

Previous investigations have found that Bcl-2 S70E affords increased protection from cytokine withdrawal-induced apoptosis compared to wt Bcl-2 (13, 14). The mechanism of this effect has been unclear. We have extended these results to other drugs such as tipifarnib and etoposide (Figs. 3B and 3C). Our demonstration that Bcl-2 S70E, like phosphorylated Bcl-2, exhibits enhanced binding to Bak and Bim (Fig. 1) provides a mechanistic explanation for increased protection by Bcl-2 S70E relative to wt Bcl-2.

Previous studies also demonstrated that Bcl-2 is phosphorylated during mitosis (8-11). The molecular consequences of this phosphorylation were not completely understood. Instead, recent investigations focused on the role of Mcl-1 as a critical regulator of apoptosis during mitosis (45). In particular, degradation of Mcl-1 by the E3 ligase FBWX7 was reported to be critical for paclitaxel-induced apoptosis. On the other hand, our results in K562 cells showed that Mcl-1 downregulation has a limited effect on paclitaxel sensitivity (Figs. 4D and S7). In contrast, Bcl-2 downregulation rendered K562 cells much more sensitive to paclitaxel-induced apoptosis, particularly at low drug concentrations (Fig. 4D and S7). Further analysis demonstrated that Bcl-2 from paclitaxel-treated cells pulls down proportionately more Bak and Bim than Bcl-2 from interphase cells (Fig. 4C). The increased affinity of phosphorylated Bcl-2 for Bak and Bim *in vitro* (Fig. 1) provides a potential explanation for these observations.

In early descriptions of ABT-737 and navitoclax, impressive synergy between these Bcl-2/Bcl-x_L antagonists and paclitaxel was reported (18, 43). We have likewise observed that navitoclax or ABT-199 increased paclitaxel-induced apoptosis in a variety of cell lines (Figs. 5 and S8). Further, we have demonstrated that the killing by the paclitaxel/navitoclax combination is markedly diminished by Bim knockdown (Fig. 5C). This synergy is not easily explained if Mcl-1 is the principal regulator of survival during mitosis but is readily explained if the mitotic phosphorylation of Bcl-2 renders this protein a particularly effective neutralizer of Bim and Bak during mitosis.

Previous studies have shown that Bcl-2 S70A, containing an alanine in place of Ser⁷⁰, also protects cell from apoptosis (12). Based on these observations, along with the assumption that phosphorylation of Ser⁷⁰ and replacement with alanine would have the opposite

functional consequences, it was concluded that phosphorylation at Ser⁷⁰ inactivates Bcl-2 (12). Accordingly, whether Ser⁷⁰ phosphorylation enhances or diminishes Bcl-2 function has been controversial. Importantly, the effects of these modifications have not previously been addressed using purified Bcl-2 under cell-free conditions. The present study shows that Bcl-2 loop phosphorylation, replacement of Ser⁷⁰ by glutamate, and replacement of Ser⁷⁰ by alanine all increase the affinity of Bcl-2 for Bak and Bim under cell-free conditions (Fig. 1) as well as the ability of Bcl-2 to sequester these proteins in intact cells (Figs. 2 and 4C).

If one assumes that phosphorylation alters Bcl-2 function by altering the charge on Ser⁷⁰, e.g., by creating or destroying a site used for interaction with a binding partner, then the similar effects of alanine and glutamate substitutions are difficult to reconcile. On the other hand, if Ser⁷⁰ is hydrogen bonded to another residue in Bcl-2, then any alteration that disrupts this hydrogen bond, including phosphorylation or replacement of the serine, might exhibit the same effect. Consistent with this latter model, we observed that S70E and S70A mutations not only had similar effects on the affinity of Bcl-2 for binding partners (Figs. 1 and 2), but also altered the conformation of the Bcl-2 flexible loop domain in a similar fashion, as indicated by protease accessibility at Arg⁶⁸ (Fig. S3). Although the Thr⁶⁹, Thr⁷⁴ and Ser⁸⁷ phosphorylation sites (Fig. S1) were not studied in as much detail, both glutamate and alanine substitutions at these sites also enhanced affinity for Bak (Fig. S2), the only binding partner examined. Once again the similar effects of alanine and glutamate substitutions are difficult to reconcile with a model that requires phosphorylation of a specific amino acid but are readily explained if these substitutions are affecting conformation of the Bcl-2 loop domain. Because this flexible loop domain has been deleted from all Bcl-2 constructs previously examined by NMR and x-ray crystallography, further structural studies are required to confirm the model described above and elucidate at the molecular level how these various modifications produce the same functional consequences.

In summary, results of the present study provide the first mechanistic explanation for the enhanced antiapoptotic effects of phosphorylated Bcl-2, demonstrate that endogenous Bcl-2 exhibits higher affinity for Bak and Bim when phosphorylated during mitosis, and provide new insight into the previously observed synergy between BH3 mimetics and paclitaxel. Interestingly, Bcl-x_L is also phosphorylated by CDK1 during mitosis (46). Moreover, the Bcl-x_L S62A mutant protects cells better than wild type Bcl-x_L against cyclin B-induced toxicity (46). Whether this phosphorylation reflects a similar mechanism for regulating Bcl-x_L function during mitosis remains to be determined.

Supplementary Material

Refer to Web version on PubMed Central for supplementary material.

Acknowledgments

The authors thank Shengbing Huang and Jin-san Zhang for Bcl-x_L and Mcl-1 shRNA plasmids and acknowledge helpful discussions with Greg Gores and Cristina Correia, assistance of Ben Madden in the Mayo Proteomics Research Core with mass spectrometry, and editorial assistance of Deb Strauss.

Grant support: This study was supported in part by R01 CA166741 and a Translational Research Program grant from the Leukemia & Lymphoma Society (6125-10).

REFERENCES

1. Martinou JC, Youle RJ. Mitochondria in apoptosis: Bcl-2 family members and mitochondrial dynamics. *Dev Cell*. 2011; 21:92–101. [PubMed: 21763611]
2. Strasser A, Cory S, Adams JM. Deciphering the rules of programmed cell death to improve therapy of cancer and other diseases. *EMBO J*. 2011; 30:3667–83. [PubMed: 21863020]

3. Chittenden T, Harrington EA, O'Connor R, Flemington C, Lutz RJ, Evan GI, et al. Induction of apoptosis by the Bcl-2 homologue Bak. *Nature*. 1995; 374:733–6. [PubMed: 7715730]
4. Willis SN, Chen L, Dewson G, Wei A, Naik E, Fletcher JI, et al. Proapoptotic Bak is sequestered by Mcl-1 and Bcl-xL, but not Bcl-2, until displaced by BH3-only proteins. *Genes Dev*. 2005; 19:1294–305. [PubMed: 15901672]
5. Llambi F, Moldoveanu T, Tait SW, Bouchier-Hayes L, Temirov J, McCormick LL, et al. A Unified Model of Mammalian BCL-2 Protein Family Interactions at the Mitochondria. *Mol Cell*. 2011; 44:517–31. [PubMed: 22036586]
6. Dai H, Meng XW, Lee S-H, Schneider PA, Kaufmann SH. Context-dependent Bcl-2/Bak Interactions Regulate Lymphoid Cell Apoptosis. *Journal of Biological Chemistry*. 2009; 284:18311–22. [PubMed: 19351886]
7. Ito T, Deng X, Carr B, May WS. Bcl-2 Phosphorylation Required for Anti-Apoptosis Function. *Journal of Biological Chemistry*. 1997; 272:11671–3. [PubMed: 9115213]
8. Ling YH, Tornos C, Perez-Soler R. Phosphorylation of Bcl-2 is a Marker of M Phase Events and Not a Determinant of Apoptosis. *Journal of Biological Chemistry*. 1998; 273:18984–91. [PubMed: 9668078]
9. Fang G, Chang BS, Kim CN, Perkins C, Thompson CB, Bhalla KN. “Loop” Domain is Necessary for Taxol-Induced Mobility Shift and Phosphorylation of Bcl-2 as Well as the Inhibiting Taxol-Induced Cytosolic Accumulation of Cytochrome C and Apoptosis. *Cancer Research*. 1998; 58:3202–8. [PubMed: 9699642]
10. Haldar S, Jena N, Croce CM. Inactivation of Bcl-2 by Phosphorylation. *Proceedings of the National Academy of Sciences of the United States of America*. 1995; 92:4507–11. [PubMed: 7753834]
11. Blagosklonny MV, Giannakou P, el-Deiry WS, Kingston DG, Higgs PI, Neckers L, et al. Raf-1/bcl-2 Phosphorylation: A Step From Microtubule Damage to Cell Death. *Cancer Research*. 1997; 57:130–5. [PubMed: 8988053]
12. Yamamoto K, Ichijo H, Korsmeyer SJ. BCL-2 is phosphorylated and inactivated by an ASK1/Jun N-terminal protein kinase pathway normally activated at G(2)/M. *Molecular and cellular biology*. 1999; 19:8469–78. [PubMed: 10567572]
13. Deng X, Ruvolo P, Carr B, May WS Jr. Survival Function of ERK1/2 as IL-3-Activated, Staurosporine-Resistant Bcl2 Kinases. *Proc Natl Acad Sci U S A*. 2000; 97:1578–83. [PubMed: 10677502]
14. Deng X, Gao F, Flagg T, May WS Jr. Mono- and multisite phosphorylation enhances Bcl2's antiapoptotic function and inhibition of cell cycle entry functions. *Proc Natl Acad Sci U S A*. 2004; 101:153–8. [PubMed: 14660795]
15. Blagosklonny MV. Unwinding the loop of Bcl-2 phosphorylation. *Leukemia*. 2001; 15:869–74. [PubMed: 11417471]
16. Furukawa Y, Iwase S, Kikuchi J, Terui Y, Nakamura M, Yamada H, et al. Phosphorylation of Bcl-2 protein by CDC2 kinase during G2/M phases and its role in cell cycle regulation. *J Biol Chem*. 2000; 275:21661–7. [PubMed: 10766756]
17. Scatena CD, Stewart ZA, Mays D, Tang LJ, Keefer CJ, Leach SD, et al. Mitotic phosphorylation of Bcl-2 during normal cell cycle progression and Taxol-induced growth arrest. *J Biol Chem*. 1998; 273:30777–84. [PubMed: 9804855]
18. Oltersdorf T, Elmore SW, Shoemaker AR, Armstrong RC, Augeri DJ, Belli BA, et al. An inhibitor of Bcl-2 family proteins induces regression of solid tumours. *Nature*. 2005; 435:677–81. [PubMed: 15902208]
19. Kutuk O, Letai A. Alteration of the mitochondrial apoptotic pathway is key to acquired paclitaxel resistance and can be reversed by ABT-737. *Cancer Res*. 2008; 68:7985–94. [PubMed: 18829556]
20. Shi J, Zhou Y, Huang HC, Mitchison TJ. Navitoclax (ABT-263) accelerates apoptosis during drug-induced mitotic arrest by antagonizing Bcl-xL. *Cancer Res*. 2011; 71:4518–26. [PubMed: 21546570]
21. Tan N, Malek M, Zha J, Yue P, Kassees R, Berry L, et al. Navitoclax enhances the efficacy of taxanes in non-small cell lung cancer models. *Clin Cancer Res*. 2011; 17:1394–404. [PubMed: 21220478]

22. Wong M, Tan N, Zha J, Peale FV, Yue P, Fairbrother WJ, et al. Navitoclax (ABT-263) reduces Bcl-x(L)-mediated chemoresistance in ovarian cancer models. *Mol Cancer Ther.* 2012; 11:1026–35. [PubMed: 22302098]
23. Hackbarth JS, Lee S- H, Meng XW, Vroman BT, Kaufmann SH, Karnitz LM. S-Peptide Epitope Tagging for Polypeptide Purification, Expression Monitoring and Localization in Mammalian Cells. *Biotechniques.* 2004; 37:835–9. [PubMed: 15560139]
24. Dai H, Smith A, Meng XW, Schneider PA, Pang Y- P, Kaufmann SH. Transient Binding of an Activator BH3 Domain to the Bak BH3-Binding Groove Initiates Bak Oligomerization. *Journal of Cell Biology.* 2011; 194:39–48. [PubMed: 21727192]
25. Svingen PA, Rodriquez J, Mesner PW Jr. Monks A, Krajewski S, Scudiero DA, et al. Components of the Cell Death Machine and Drug Sensitivity of the NCI Cell Line Panel. *Clin Cancer Res.* 2004; 10:6807–20. [PubMed: 15501957]
26. Huang S, Sinicrope FA. Celecoxib-induced apoptosis is enhanced by ABT-737 and by inhibition of autophagy in human colorectal cancer cells. *Autophagy.* 2010; 6:256–69. [PubMed: 20104024]
27. Kaufmann SH. Reutilization of Immunoblots After Chemiluminescent Detection. *Analytical Biochemistry.* 2001; 296:283–6. [PubMed: 11554725]
28. Meng XW, Lee SH, Dai H, Loegering D, Yu C, Flatten K, et al. Mcl-1 as a buffer for proapoptotic Bcl-2 family members during TRAIL-induced apoptosis: a mechanistic basis for sorafenib (Bay 43-9006)-induced TRAIL sensitization. *J Biol Chem.* 2007; 282:29831–46. [PubMed: 17698840]
29. Smith PK, Krohn RI, Hermanson GT, Mallia AK, Gartner FH, Provenzano MD, et al. Measurement of Protein Using Bicinchoninic Acid. *Analytical Biochemistry.* 1985; 150:76–85. [PubMed: 3843705]
30. Matthews, DE.; Farewell, VT., editors. *Using and Understanding Medical Statistics.* 2nd ed.. Karger; Basel: 1988.
31. Jason-Moller L, Murphy M, Bruno J. Overview of Biacore systems and their applications. *Curr Protoc Protein Sci.* 2006 Chapter 19:Unit 19 3.
32. Berggard T, Linse S, James P. Methods for the detection and analysis of protein-protein interactions. *Proteomics.* 2007; 7:2833–42. [PubMed: 17640003]
33. Haldar S, Basu A, Croce CM. Serine-70 is one of the critical sites for drug-induced Bcl2 phosphorylation in cancer cells. *Cancer Res.* 1998; 58:1609–15. [PubMed: 9563469]
34. Ruvolo PP, Deng X, May WS. Phosphorylation of Bcl2 and regulation of apoptosis. *Leukemia.* 2001; 15:515–22. [PubMed: 11368354]
35. O'Connor L, Strasser A, O'Reilly LA, Hausmann G, Adams JM, Cory S, et al. Bim: a novel member of the Bcl-2 family that promotes apoptosis. *EMBO Journal.* 1998; 17:384–95. [PubMed: 9430630]
36. Bouillet P, Metcalf D, Huang DC, Tarlinton DM, Kay TW, Kontgen F, et al. Proapoptotic Bcl-2 Relative Bim Required for Certain Apoptotic Responses, Leukocyte Homeostasis, and to Preclude Autoimmunity. *Science.* 1999; 286:1735–8. [PubMed: 10576740]
37. Merino D, Giam M, Hughes PD, Siggs OM, Heger K, O'Reilly LA, et al. The role of BH3-only protein Bim extends beyond inhibiting Bcl-2-like prosurvival proteins. *Journal of Cell Biology.* 2009; 186:355–62. [PubMed: 19651893]
38. Petros AM, Medek A, Nettlesheim DG, Kim DH, Yoon HS, Swift K, et al. Solution structure of the antiapoptotic protein bcl-2. *Proc Natl Acad Sci U S A.* 2001; 98:3012–7. [PubMed: 11248023]
39. Ku B, Liang C, Jung JU, Oh BH. Evidence that inhibition of BAX activation by BCL-2 involves its tight and preferential interaction with the BH3 domain of BAX. *Cell Res.* 2011; 21:627–41. [PubMed: 21060336]
40. Rupley, JA. Susceptibility to attack by proteolytic enzymes.. In: Hirs, CHW., editor. *Enzyme Structure.* Academic Press; New York: 1967. p. 905-17.
41. Ding H, Hackbarth J, Schneider PA, Lee S- H, Meng XW, Dai H, et al. Cytotoxicity of Farnesyltransferase Inhibitors in Lymphoid Cells Mediated by MAPK Pathway Inhibition and Bim Upregulation. *Blood.* 2011:4872–81. [PubMed: 21673341]
42. Losiewicz MD, Carlson BA, Kaur G, Sausville EA, Worland PJ. Potent Inhibition of CDC2 Kinase Activity by the Flavonoid L86-8275. *Biochemical and Biophysical Research Communications.* 1994; 201:589–95. [PubMed: 8002990]

43. Tse C, Shoemaker AR, Adickes J, Anderson MG, Chen J, Jin S, et al. ABT-263: a potent and orally bioavailable Bcl-2 family inhibitor. *Cancer Res.* 2008; 68:3421–8. [PubMed: 18451170]
44. Souers AJ, Levenson JD, Boghaert ER, Ackler SL, Catron ND, Chen J, et al. ABT-199, a potent and selective BCL-2 inhibitor, achieves antitumor activity while sparing platelets. *Nat Med.* 2013
45. Wertz IE, Kusam S, Lam C, Okamoto T, Sandoval W, Anderson DJ, et al. Sensitivity to antitubulin chemotherapeutics is regulated by MCL1 and FBW7. *Nature.* 2011; 471:110–4. [PubMed: 21368834]
46. Terrano DT, Upreti M, Chambers TC. Cyclin-dependent kinase 1-mediated Bcl-xL/Bcl-2 phosphorylation acts as a functional link coupling mitotic arrest and apoptosis. *Molecular and cellular biology.* 2010; 30:640–56. [PubMed: 19917720]
47. Blajeski AL, Phan VA, Kottke TJ, Kaufmann SH. G1 and G2 Arrest Following Microtubule Depolymerization in Human Breast Cancer Cells. *Journal of Clinical Investigation.* 2002; 110:91–9. [PubMed: 12093892]
48. Mesa RA, Loegering D, Powell HL, Flatten K, Arlander SAH, Dai NT, et al. Heat Shock Protein 90 Inhibition Sensitizes Acute Myelogenous Leukemia Cells to Cytarabine. *Blood.* 2005; 106:318–27. [PubMed: 15784732]
49. Nicoletti I, Migliorati G, Pagliacci MC, Grignani F, Riccardi C. A Rapid and Simple Method for Measuring Thymocyte Apoptosis by Propidium Iodide Staining and Flow Cytometry. *J Immunol Methods.* 1991; 139:271–9. [PubMed: 1710634]

PRÉCIS

Findings offer a mechanistic basis to understand the enhanced anti-apoptotic activity of phosphorylated Bcl-2, along with the ability of BH3 mimetics to enhance cancer cell sensitivity to taxanes.

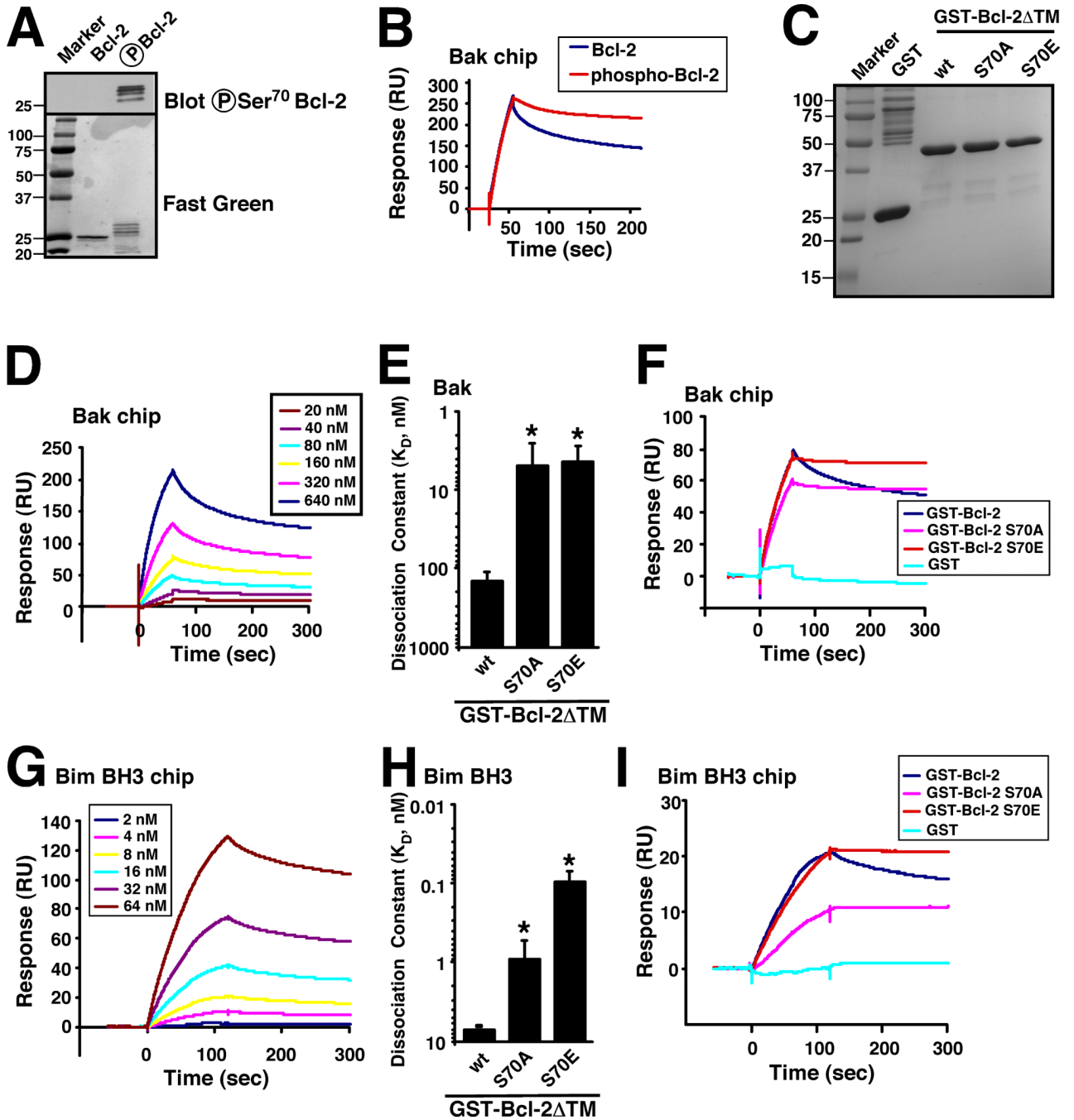


Figure 1. Bcl-2 phosphorylation or Ser⁷⁰ mutation enhances interaction with Bak and Bim
A, after purified Bcl-2 Δ TM-His₆ was phosphorylated by CDK1/cyclin B *in vitro* (see Methods), the mixture was separated by SDS-PAGE, transferred to nitrocellulose, stained with fast green FCF, or blotted with anti-phospho-Ser⁷⁰-Bcl-2 antibody. **B**, using the same chip, the binding of 160 nM unphosphorylated or CDK1/cyclin B-phosphorylated Bcl-2 Δ TM-His₆ to immobilized Bak Δ TM was compared. Phosphorylation of Bcl-2 Δ TM-His₆ is documented in Fig. S1. **C**, Coomassie blue staining of purified GST, GST-Bcl-2 Δ TM was well as the S70A and S70E mutants. **D**, surface plasmon resonance (relative units) observed when immobilized Bak Δ TM was exposed to different concentrations of GST-

Bcl-2 Δ TM. **E**, based on the surface plasmon resonance assay, the affinities of wt, S70A and S70E Bcl-2 Δ TM for Bak were calculated. *, $p < 0.004$ vs. control by ANOVA. **F**, binding of 160 nM GST-Bcl-2 Δ TM (wt, S70A, or S70E) vs. GST to immobilized Bak Δ TM was compared using the same chip. **G**, surface plasmon resonance (relative units) observed when immobilized Bim BH3 peptide was exposed to different concentrations of GST-Bcl-2 Δ TM. **H**, based on the surface plasmon resonance assay, the affinities of Bcl-2 (wt, S70A and S70E) for Bim BH3 were calculated. *, $p < 0.001$ vs. control by ANOVA. **I**, binding of 8 nM GST-Bcl-2 Δ TM (wt, S70A, or S70E) vs. GST to immobilized Bim BH3 peptide was compared. Error bars in panels E and H, \pm SD of three independent experiments.

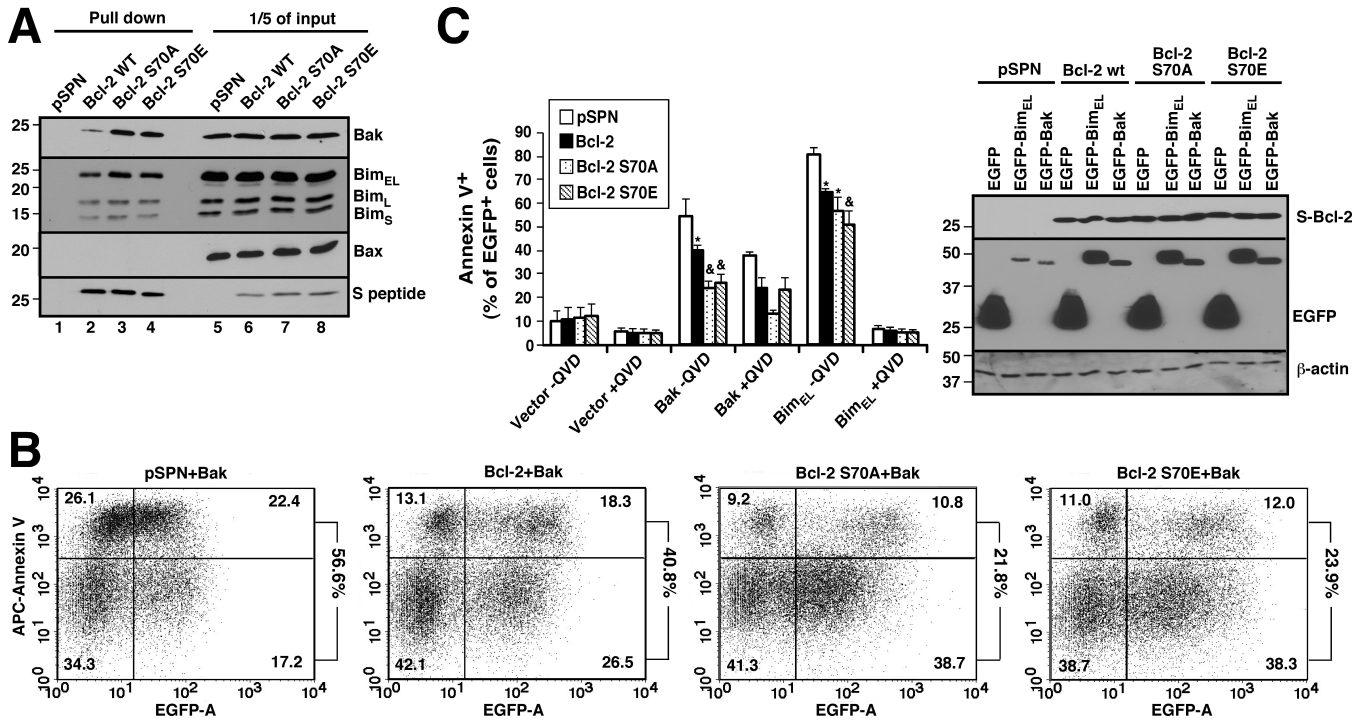


Figure 2. Bcl-2 Ser⁷⁰ modifications increase cellular resistance to Bak- or Bim-induced apoptosis
A, 24 h after Jurkat cells were transiently transfected with S-tagged Bcl-2 (wt, S70A or S70E), cell lysates prepared in isotonic buffer containing 1% CHAPS were reacted with S protein-agarose to recover Bcl-2. Pulldowns and 1/5 of the inputs were probed with the indicated antibodies. **B, C**, after transfection with 20 μg EGFP-C1 (control), EGFP-Bim_{EL} or EGFP-Bak together with 20 μg pSPN or pSPN encoding Bcl-2 (wt, S70A or S70E), K562 cells were incubated for 24 h in the presence or absence of 5 μM QVD-OPh and stained with APC-annexin V. Panel B shows dot plots from one experiment. Numbers at right indicate percentage of EGFP⁺ cells that are also annexin V⁺. Panel C summarizes results from three independent experiments. Error bars, ± SD. *, *p* < 0.02 vs. empty vector; &, *p* < 0.03 (Bak) or *p* < 0.003 (Bim) vs. wt Bcl-2 and *p* < 0.003 vs. empty vector. **Inset in C**, cell lysates were subjected to SDS-PAGE and probed with antibodies to the indicated antigens to confirm equal transgene expression.

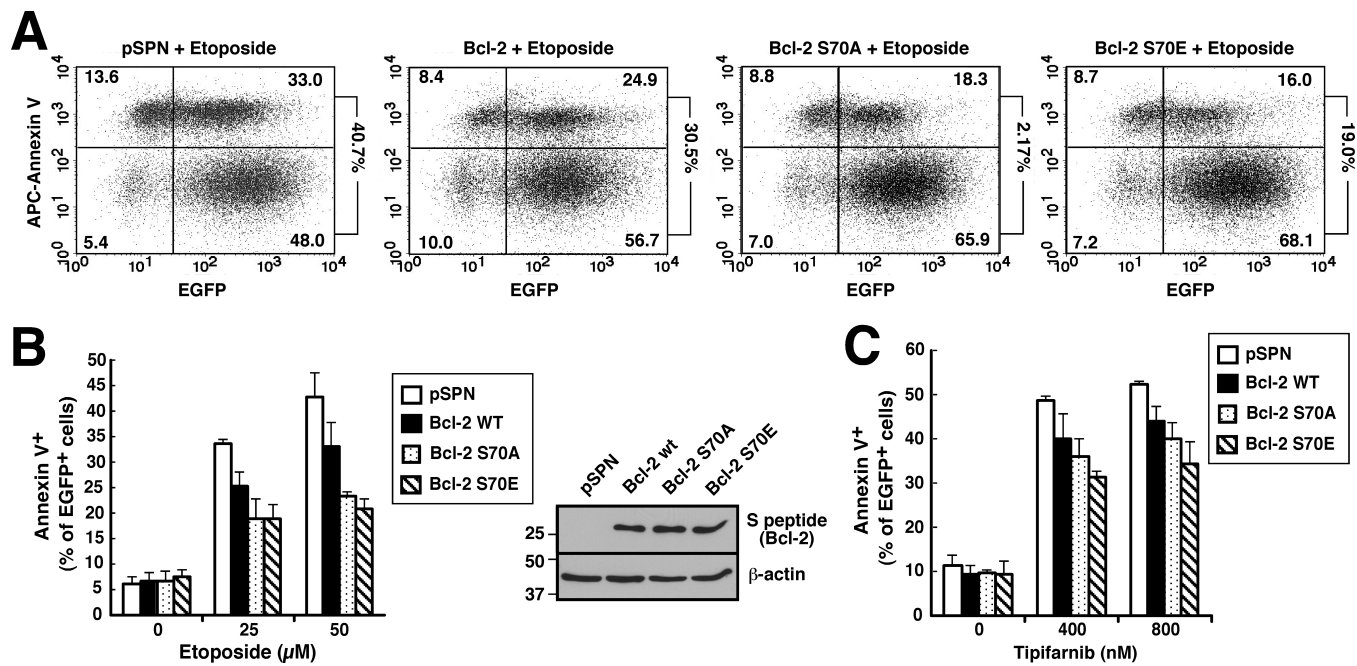


Figure 3. Bcl-2 S70A and S70E both diminish drug-induced apoptosis

Beginning 24 h after Jurkat cells were transfected with 40 μ g pSPN or S peptide-tagged Bcl-2 (wt, S70A or S70E) together with 5 μ g plasmid encoding EGFP-Histone H2B, cells were treated with the indicated concentrations of etoposide for 7 h (A, B) or tipifarnib for 72 h (C), then stained with APC-annexin V. The percentage of EGFP⁺ cells that stained with annexin V is indicated at the right of each dot plot in panel A and summarized in panel B. Error bars in B and C, \pm SD of three independent experiments. **Inset in B**, cell lysates were subjected to SDS-PAGE and probed with the indicated antibodies to confirm equal expression of Bcl-2 constructs.

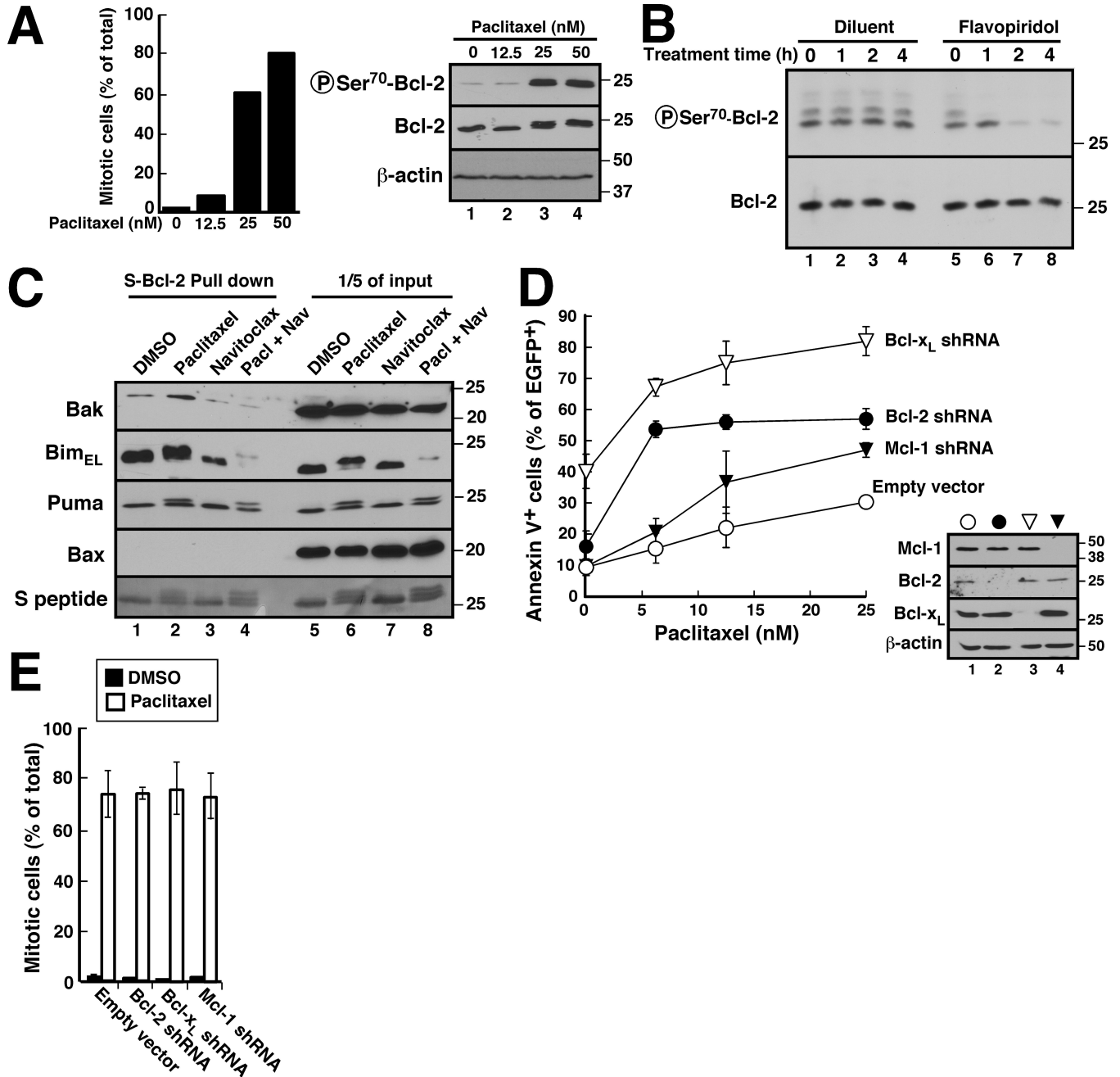


Figure 4. Effect of Bcl-2 phosphorylation on paclitaxel sensitivity

A, 18 h after K562 cells were treated with indicated paclitaxel concentration, cells were stained with Hoechst 33258 and viewed by fluorescence microscopy (left) for mitotic cells (47) or subjected to SDS-PAGE and probed with the indicated antibodies (right). **B**, after K562 cells were treated with 25 nM paclitaxel for 16 h, diluent (lanes 1-4) or 300 nM flavopiridol (lanes 5-8) was added for the indicated length of time in the continued presence of paclitaxel. Whole cell lysates were then subjected to SDS-PAGE and probed with the indicated antibodies. **C**, 24 h after K562 cells stably expressing S peptide-tagged Bcl-2 were treated with diluent, 25 nM paclitaxel, 1 μM navitoclax or 25 nM paclitaxel + 1 μM navitoclax, cell lysates prepared in 1% CHAPS buffer were incubated with S protein-agarose to recover Bcl-2 complexes. After SDS-PAGE and transfer to nitrocellulose,

pulldowns (lanes 1-4) and 1/5 of the inputs (lanes 5-8) were probed with the indicated antibodies. **D**, 24 h after K562 cells were transiently transfected with empty vector, PCMS5A-Bcl-2 shRNA, PCMS5A-Bcl-x_L shRNA or PCMS5A-Mcl-1 shRNA (all with EGFP-histone H2B expression), cells were treated with paclitaxel for another 48 h, and stained with APC-annexin V. The percentage of EGFP⁺ cells that stained with annexin V is indicated. **Inset in D**, immunoblots showing knockdown of the targeted protein. **E**, mitotic indices of cells transfected with the constructs described in panel D, incubated for 24 h to allow protein knockdown, and treated with paclitaxel or diluent for an additional 18 h. Error bars in D and E, \pm SD of three independent experiments.

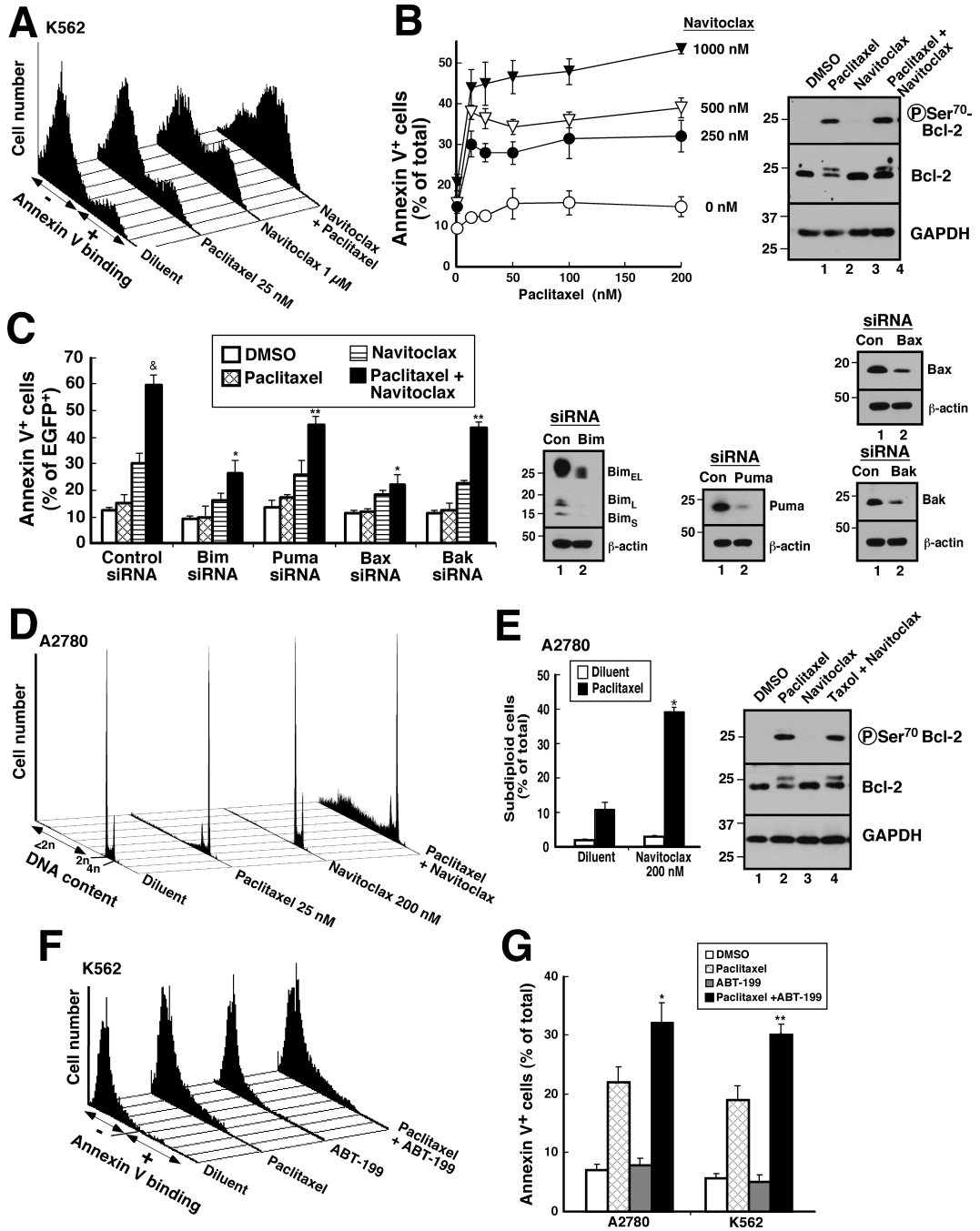


Figure 5. Navitoclax acts in part through Bcl-2 to enhance paclitaxel-induced apoptosis
A, B, 24 h after K562 cells were treated with the indicated concentrations of paclitaxel with or without indicated concentrations of navitoclax, cells were stained with APC-annexin V. Histograms from one experiment (A) and summarized results from 3 independent experiments (B) are shown. **Inset in B,** immunoblots probed with antibodies to the indicated antigen. **C,** 24 h after K562 cells were transfected with control siRNA or siRNAs targeting Bim, Puma, Bak, or Bax together with EGFP-Histone H2B plasmid, cells were treated with 25 nM paclitaxel, 1 μM navitoclax or 25 nM paclitaxel + 1 μM navitoclax for another 24 h, then stained with APC-annexin V. &, *p* < 0.01 by ANOVA vs. other treatments of cells

transfected with control siRNA. *, $p < 0.001$ vs. control siRNA treated with paclitaxel + navitoclax and $p < 0.006$ vs Puma siRNA or Bak siRNA treated with the combination. **, $p < 0.002$ vs. control siRNA treated with the combination. **Inset in C**, immunoblots were probed with antibodies to the indicated antigen. **D, E**, 24 h after A2780 cells were treated diluent or paclitaxel, with or without navitoclax, cells were stained with PI under conditions where fragmented chromatin is extracted (48, 49) and examined for DNA content. DNA histograms from one experiment (D) and summarized results from 3 independent experiments (E) are shown. *, $p < 0.001$ by ANOVA vs. paclitaxel alone or other treatment. **Inset in E**, immunoblots showing whole cell lysates probed for the indicated antigens. **F, G**, 48 h after A2780 and K562 cells were treated with diluent or paclitaxel (25 nM) with or without ABT-199 (1 μ M), cells were stained with APC-annexin V. Histograms from one experiment in K562 (F) and summarized results from 3 independent experiments in both cell lines (G) are shown. *, **, $p < 0.002$ and 0.09, respectively vs. paclitaxel alone by ANOVA. Error bars in B, C, E, G, \pm SD of 3 independent experiments.